Electroanalytical Assessment of the Oxygen Permeability at the Gas-Solid-Liquid Interface in Polymer-based Materials for Lens Applications

Ahmed Jarboui, Yaovi Holade, Jean-Pierre Mericq, Christophe Charmette, Thierry Thami, Peter Biermans, Sophie Tingry, Denis Bouyer

Electroanalytical Assessment of the Oxygen Permeability at the Gas-Solid-Liquid Interface in Polymer-based Materials for Lens Applications

Ahmed Jarboui[a], Yaovi Holade[a], Jean-Pierre Mericq*[a], Christophe Charmette[a], Thierry Thami[a], Peter Biermans[b], Sophie Tingry*[a], Denis Bouyer[a]

[a] A. Jarboui, Dr. Y. Holade, Dr. J.-P. Mericq, Dr. C. Charmette, Dr. T. Thami, Dr. S. Tingry, Pr. Denis Bouyer
Institut Européen des Membranes
IEM UMR 5635, Univ Montpellier, ENSCM, CNRS, Montpellier, France
E-mail: sophie.tingry@umontpellier.fr
jean-pierre.mericq@umontpellier.fr

[b] P. Biermans
Ophtimalia
5 esplanade Anton Philips Campus EffiScience, 14460 Colombelles, France.

Abstract. The design of efficient electrochemical setups to precisely and timely quantify the oxygen permeability, which dictates how the lens let O_2 to reach the eye, is important for the development lens-based materials. We report herein a home-made electro-analytical platform made of a 3D-printed diffusion electrochemical cell to assess this parameter. The design overcomes edge effects and allows analysis under conditions similar to lens wear where the liquid is in contact to the inner surface while the gaseous O_2 is in contact with the outer surface. The testing of three types of contact lens materials (flexible polymer, rigid polymer, and gel-type) showed that the O_2 permeability can be fairly well evaluated by the chronoamperometry study of oxygen reduction reaction. Under conditions similar to those of lens wear, our findings showed that the measurement error was 6%, which offer an alternative to the classic gas-to-gas method for O_2 permeability determination.

Introduction

Oxygen permeability (Perm) is an important decision-maker parameter for the development of materials used in the fabrication of contact and scleral lenses.[1] This parameter represents the ease for oxygen to diffuse through the lens to reach the cornea. Permeability depends on the oxygen diffusion *D* and the oxygen solubility *k* and can then be written as Perm = *D*×*k* usually expressed in barrer unit. A low permeability material can lead to various complications such as bacterial infection,[2] swelling[3] and vascularization[4] due to the limited oxygen flux that reaches the corneal cells. Specifically, the accurate evaluation of this property allows the identification of strategies to be implemented to improve the design and development of suitable polymer materials of which the lenses are made. Hence, measuring accurately the oxygen permeability of lens materials is therefore of a great importance prior to a biomedical testing.[5]

There are several methods for measuring oxygen permeability such as the gas-to-gas and electrochemical methods performed in aqueous media.[6] The gas-to-gas method[7] is a well-established approach that has been standardized by the American Society for Testing and Materials (ASTM) for use in the packaging industry.[8] It measures the amount of oxygen that passes through a sample using pressure sensors. The main issue when using this method for permeability measurements on rigid lens material is the low oxygen flux through the sample due to the small diameter and high thickness of industrial lenses. More sensitive methods have therefore to be developed for measuring small amounts of oxygen, and the electrochemical methods parade as a viable alternative. Indeed, owing to their characteristics of high sensitivity, selectivity, response time, and reusability, electrochemical methods represent a sustainable strategy for qualitative and quantitative analysis of a specific analyte in a given biological matrix. An electrochemical method in this case consists of measuring the oxygen reduction reaction (ORR) current at the surface of an electrode, which is a well-known reaction in electrochemistry for the first generation of biosensors for glucose sensing[9] and in fuel cells for electrical energy production.[10] So, a specific electrode that is situated close to the lens will be able to detect and quantify any dissolved oxygen from the overall process $O_{2(dis)} + 4H^+_{(aq)} + 4e^- \rightarrow 2H_2O_{(l)}$. To date, the standard polarography method or the so-called “Fatt method” was firstly introduced by Fatt[11] and requires the presence of a layer of water between the surface of the sample and the electrode for the dissolved oxygen to be reduced. The water layer consists of a thin wet paper inserted between the sample and the cathode to ensure diffusion and reduction of oxygen at the cathode surface. This wet paper induces an additional diffusion resistance which must not be negligible compared to that of the sample and taken into account when calculating oxygen permeability. A partial solution to this problem was to calculate the oxygen diffusion resistance of the water layer by varying the thickness of either the samples or the thin wet paper.[12] It should also be noted that the Fatt method may be applied only for samples with a permeability up to 100 barrer and for thin samples (0.4 mm) due to boundary resistance and edge effects[13] caused by lateral diffusion. Several solutions have been proposed to eliminate the edge effect such as using thin samples or cathodes divided by narrow insulations. Wichterlova *et al*.[13] proposed a modified polarography method using an inert gas to minimize lateral diffusion and reduce the edge effects. However, it should be noted that the efficient determination of oxygen permeability by electrochemical methods of the emerged flexible and rigid polymer-based materials for contact lens applications is still a great challenge.

In this work, we report a new electrochemical setup to accurately evaluate the oxygen permeability in a close contact lens applications conditions. The strategy integrated a fabricated 3D printed diffusion cell, the electrochemical oxygen reduction reaction, and the chronoamperometry technique to efficiently determine the oxygen permeability of flexible polymer, rigid polymer, and gel-type materials under conditions similar to lens wear. The effects of the measurement conditions such as the gas pressure, the electrolyte stirring, and the wet/dry state were thoroughly scrutinized. Oxygen permeability measured by the chronoamperometry method was also compared to permeability values measured by the classic gas-to-gas (or time-lag) method.

Results and Discussion

Designed 3D printed diffusion electrochemical cell

A home-made 3D printed diffusion cell was constructed for the purpose of oxygen permeability evaluation by an electrochemical method. Figures 1a and 1b display the cell composed of two compartments, liquid and gas units. The polymer sample is fixed between the two chambers using an O-ring made of silicone based joint material to ensure perfect sealing. The inner surface of the O-ring is a disc of 10 mm diameter. Pt working electrode (1.6 mm diameter), a silver counter electrode (3 mm diameter), and Ag|AgCl|NaCl 3 M (referred to as Ag/AgCl) reference electrode were immersed in the liquid (volume = 9 mL) consisting of a 0.02 M phosphate buffer saline solution (PBS). A magnetic stirrer is placed on the inner surface of the sample for the electrolyte homogenization (no stirring during chronoamperometry). The volume of the liquid chamber has been optimized to the minimum taking into account the dimensions of the electrodes. The distance between the electrodes is about 0.4 cm and they are 1.5 cm away from the magnetic stirrer. Oxygen under pressure passes through the sample and reaches the electrolyte where it is immediately and homogenously distributed in the solution. The diffusion cell is placed in a temperature-controlled chamber at 35 ± 1 °C to mimic the temperature of the eye surface.

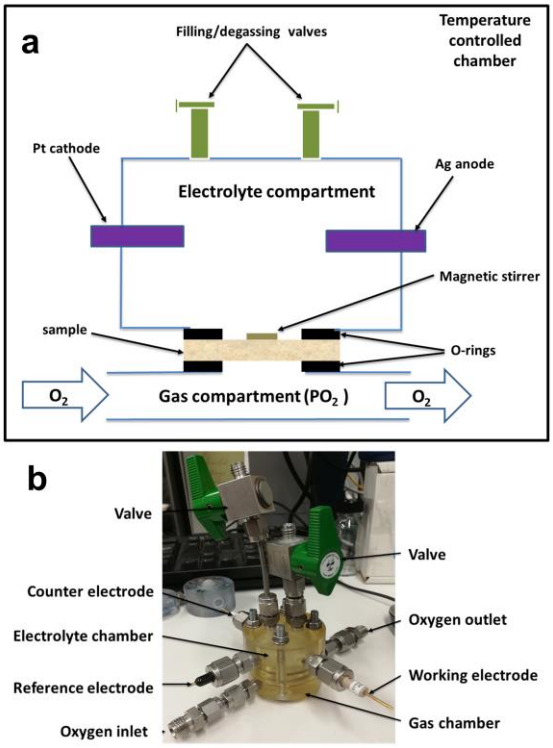

Figure 1. (a) 2D scheme of the targeted 3D-printed cell to evaluate the oxygen permeation, Ag/AgCl reference electrode is not shown. (b) Picture of the cell.

Determination of the oxygen solubility

Before measuring the oxygen permeability of the samples, the oxygen solubility was first measured in pure water and in PBS, used as electrolyte in our study, to validate the measurement method. To this end, the solutions were aerated directly by a flow of pure oxygen (10 mL min^{-1}) through the filling valves and the current from ORR was evaluated in order to calculate the soluble oxygen concentration as a function of time. Figure 2 shows the increase of oxygen concentration (see Experimental Section for the calculation) that reaches saturation after 100 min. It is worth of mentioning that for a routine electrochemical experiment of oxygen reduction reaction, O_2 is directly bubbled in the electrolyte to facilitate the hydration and hence maximized the amount of dissolved oxygen in a short time of 10 to 30 min depending on the cell total volume and type of solution (time increases with the pH). So it was expected to find here a duration higher than a typical time scale because it is impossible to directly bubble in the liquid chamber, which would not reflect the reality of contact lens application (see Figure 1).

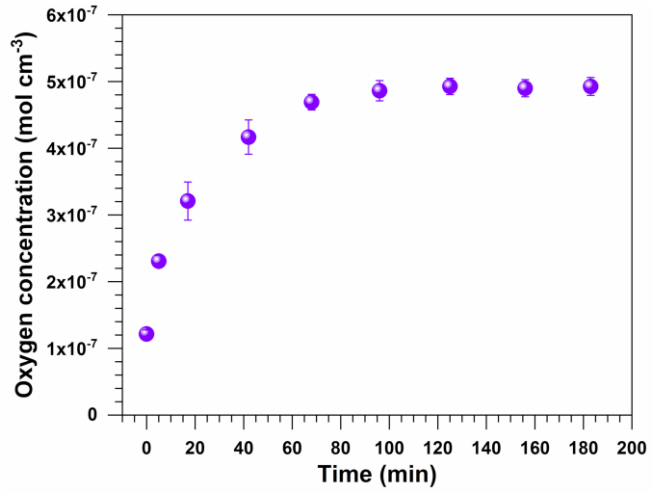

Figure 2. Evolution of the oxygen concentration as the function of the time at 35 °C in PBS aerated directly by a flow of pure oxygen (10 mL min^{-1}) at 1 bar.

The determined maximum oxygen concentration of 5.0×10^{-7} mol cm^{-3} (= 5.0×10^{-4} mol L^{-1} = 0.5 mM) at a pressure of 1 bar (the second degassing valve is kept open) is in the range of reported value of 0.2-0.5 mM of soluble O_2 in equilibrium with air in PBS-based biological conditions.[14] It should be noted that the control experiment in water (presence of inorganic salt (NaCl) with concentration of about 0.02 M such as PBS) gave a value of $1.2\times10^{-6} \pm 1\times10^{-7}$ mol cm^{-3} (= $1.2\times10^{-3} \pm 1\times10^{-4}$ mol L^{-1} = 1.2 ± 0.1 mM), which is in agreement with the widely used value of $1.1\text{-}1.2\times10^{-6}$ mol cm^{-3} as the bulk concentration of O_2 in the "clean aqueous electrolyte" obtained by dissolution of simple inorganic compound in pure water.[15] Those results allow us to validate our setup. The variation of the oxygen solubility in liquids depends on the temperature, O_2 pressure at the water surface and other types of dissolved species, decreasing at higher temperature and higher electrolyte concentration, and increasing at higher pressure.[15b] In water, the value goes from 1.39×10^{-6} mol cm^{-3} at 20 °C to 1.04×10^{-6} mol cm^{-3} at 40 °C (1.013 bar of O_2 pressure), and decreases with salinity from 0.216×10^{-6} mol cm^{-3} at 0 salinity to 0.091×10^{-6} mol cm^{-3} at 133.15 salinity at 35 °C and atmospheric O_2 pressure.[15b,16]

Influence of the experimental conditions on the permeability measurement

We next aimed to carefully study the impact of the oxygen pressure in the gas chamber and the stirring of the electrolyte, in order to evaluate their contribution on the value of O_2 permeability. The oxygen pressure has an impact on the oxygen flow through the sample, while the stirring speed decreases the resistance to oxygen transfer through the electrolyte layer to the electrode surface. Permeability measurements have been first performed with the polymer material so-called Roflufocon D of CONTAMAC in its Optimum Extra version. Figure 3a shows the influence of the oxygen pressure in the gas chamber. O_2 concentration increases with a faster rate in the electrolyte compartment for the measurements performed at 3 bar. Quantitatively, the O_2 concentration rate is 2.58×10^{-9} mol cm^{-3} min^{-1} at 1.5 bar compared to 5.5×10^{-9} mol cm^{-3} min^{-1} at 3 bar.

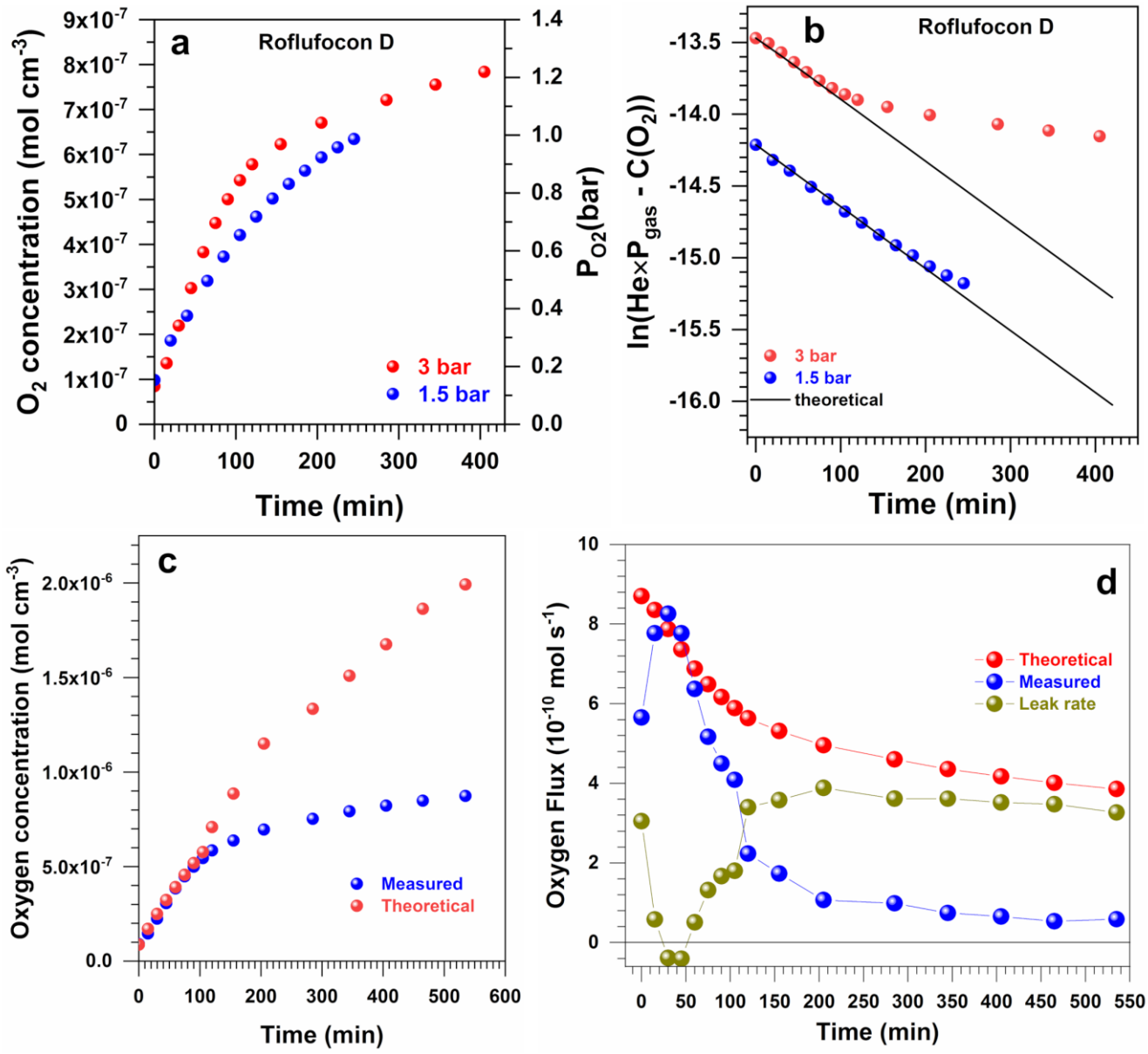

Figure 3. Study of the Roflufocon D sample. Variation of (a) O_2 concentration (left *y*-axis) and calculated PO_2 (right *y*-axis), and (b) $\ln(He*P_{gas} - C(O_2))$ as a function of time at P_{gas} = 1.5 and 3 bar in the oxygen gas compartment at 35 °C: The theoretical line corresponds to the part of the curve extended over the entire measuring range and used to calculate the permeability. Measured and theoretical estimation of O_2 leak rate at P_{gas} = 3 bar and 35 °C in terms of (c) the concentration and (d) the flux..

In Figure 3b, the variation of $\ln(He*Pair - C(O_2))$ is linear up to t = 75 min and then deviates from the initial linear behavior. The same behavior is noticed for the measurement at 1.5 bar but at a longer time of 205 min. For both experimental conditions, referring to Figure 3a, the deviation from the linear behavior occurs at an oxygen partial pressure of 0.9 bar. This deviation can be explained by a possible gas leakage from the electrolyte chamber when the oxygen partial pressure increases above 0.9 bar. For this reason and in order to prevent under estimation of the permeability of the characterized samples, only the slope obtained from the low time values (t < 100 min) was taken into account for the measurements performed with Roflufocon D material. The difference in starting value (at t = 0) between the measurements at 3 bar and 1.5 bar is only due to the difference in the initial oxygen concentration in the electrolyte compartment. It is therefore preferable to work at a lower pressure in order to avoid a rapid increase in pressure in the electrolyte compartment and to minimize any leakage. However, in the case of a low permeability material, a higher pressure will be necessary to ensure sufficient oxygen flow to have an accurate measurement of permeability.

To get insights about the above limiting point and to know which period of time enables determining correctly the oxygen permeability, we next designed a model for quantifying the oxygen leak flux. Typically, the leakage occurs when the chamber where the oxygen concentration increases is isolated

from the ambient air, as in the case of the gas-to-gas method[7] and is mainly due to the design of the diffusion cell (presence of valves, sensors or electrodes connections). In our case, the leakage of gas out of the electrolyte chamber is possible at the connections between the rings holding the materials in place, the electrodes connections to the liquid chamber and from the connections of the degassing valves. The oxygen flux ($FO_{2measured}$) was calculated using the oxygen concentration measured experimentally as shown in Eq. 1, while the theoretical value of the oxygen flux was calculated using the permeability value (Eq. 2). Then, the leak rate was calculated as the difference between the measured and the calculated oxygen flux (Eq. 3). Hence the calculated oxygen concentration variation in the electrolyte solution can be deducted from Eq. 4. The experimentally measured and theoretically calculated sets of data are presented in Figures 3c and 3d. For the investigated materials of example of the Roflufocon D with Dk = 86 barrer and 730 µm thicknesses, the oxygen flux into the electrolyte chamber is at its maximum of 8.2×10^{-10} mol s^{-1} for 30-60 min and then decreases with time when the oxygen concentration increases within the electrolyte chamber due to the decrease in driving force. The leak rate is minimal below 100 min and then becomes significant (Figure 3c). For the measurements performed below 100 min (corresponding to a dissolved oxygen concentration of 5.2×10^{-7} mol cm^{-3}), the calculated and measured concentration values overlapped (Figure 3d). However, when the oxygen concentration increases higher than this value, the measured oxygen concentration is lower than the calculated value. This means that there is an oxygen loss at higher oxygen concentration in the electrolyte chamber. Hence only the data where the measured and calculated oxygen concentration overlaps will be further used in the next sections to fairly calculate the oxygen permeability. The higher value of the leak rate calculated at t = 0 min is only due to the time-lag between the start of the measurement and oxygen diffusion through the sample thickness so that no oxygen has reached the electrolyte yet. The leakage rate can be reduced or delayed in time (to have sufficient data points for permeability calculation) by using a decreased oxygen concentration in the gas compartment for average and high permeability samples. For samples with low oxygen permeability, maintaining high oxygen pressure at the gas compartment is preferable to have sufficient oxygen flux to the electrolyte compartment.

$$FO_{2measured} = \frac{C_{O2}(n) - C_{O2}(n-1)}{t_n - t_{n-1}} V_{PBS} \quad \text{(Eq. 1)}$$

$$FO_{2theoretical} = Perm\left(P_{gas} - \frac{C_{O2}(n)}{He)}\right) S_{transfer} \quad \text{(Eq. 2)}$$

$$FO_{2leak} = FO_{2theoretical} - FO_{2measured} \quad \text{(Eq. 3)}$$

$$CO_{2theoretical} = FO_{2theoretical}\left(t_n - t_{n-1}\right)\frac{1}{V_{PBS}} \quad \text{(Eq. 4)}$$

Where $FO_{2measured}$(in mol s^{-1}) is the measured oxygen flux, $FO_{2theoretical}$(in mol s^{-1}) is the calculated oxygen flux, V_{PBS}(in cm^3) is the electrolyte volume, C_{O2}(n) is the oxygen concentration at the time t_n, $S_{transfer}$(in cm^2) is the sample surface exposed to oxygen, Perm(in mol bar^{-1} cm^{-1} s^{-1}) is the oxygen permeability, FO_{2leak}(in mol s^{-1}) is the leak rate.

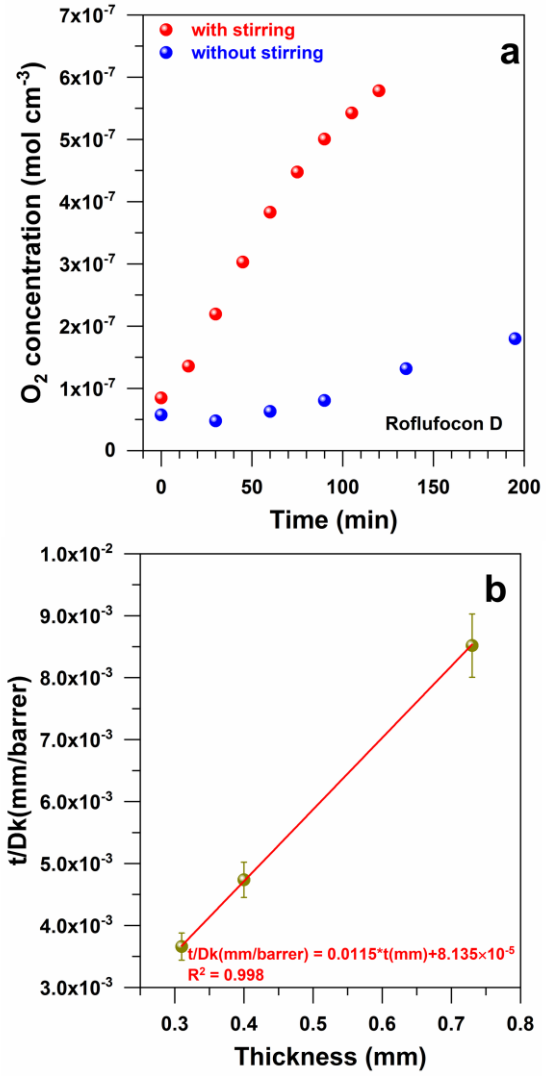

Figure 4. (a) Variation of the measured oxygen concentration as a function of time when the solution was preliminary stirred or not for the Roflufocon D sample at 3 bar and 35°C. (b) Oxygen transfer resistance as a function of the Roflufocon D sample thickness to determine electrolyte resistance.

As mentioned above, the electrolyte stirring before any chronoamperometry experiment is an important parameter and should be performed adequately so that the diffusion resistance of the electrolyte layer can be suppressed or at least minimized to a negligible value compared to mass transfer resistance of the samples to oxygen diffusion. As indicated above, O_2 cannot be directly bubbled in the solution such a classic electrochemical experiment of oxygen reduction reaction (10-30 min). So it was necessary to find a strategy to augment the contact between the gaseous O_2 and the electrolyte as it would happen in practical application of contact lens with the interstitial fluid to facilitate the hydration and hence maximized the amount of dissolved O_2. Figure 4a compares experiments performed on the Roflufocon D sample at 3 bar with and without the electrolyte stirring. A 3 bar pressure in the gas compartment was chosen here in order to have a measurable increase of the O_2 concentration in the electrolyte compartment for the non-stirred solution. No noticeable damage to the sample surface during magnetic stirring of the electrolyte was observed by SEM analysis (results

not shown). In the case of the stirred solution, the oxygen permeability was calculated by limiting the time of the experiment to 100 min in order to prevent permeability underestimation due to possible leaks. As expected, the measured O_2 concentration increases remarkably faster in the case of electrolyte stirring than that in the case of unstirred electrolyte. In the 3D-printed electrochemical diffusion cell used in this work, oxygen diffuses through the sample and then through the electrolyte solution to reach the electrode surface where the oxygen reduction reaction occurs (see Figure 1). The thickness of the polymer sample is 500 µm, while the distance between the surface of the sample and the surface of the working electrode is 1.5 cm, which can result in a difference in thickness that is 30 to 40 times smaller when considering the investigated material alone. Under this condition, the resistance of the electrolyte to oxygen transfer will be considerably higher than that of the sample if there is no agitation, limiting the measured permeability range to values below that of oxygen in the stirred electrolyte by at least 30-40 times.

Having demonstrated the importance of a preliminary stirring of the solution for the determination of the oxygen permeability, the electrolyte resistance was estimated. The total oxygen transfer resistance (t/Dk) is a combination in series of the electrolyte resistance and the sample resistance (Eq. 5). The resistance of the electrolyte to transfer is constant at a fixed stirring speed. Thus, performing permeability measurements using the same Roflufocon D polymer sample with different thicknesses allows evaluating the resistance of the solution to be determined by extrapolation of the intersection of the straight line with the *y*-axis. From Figure 4b, the value of the electrolyte resistance to oxygen transfer at a fixed stirring speed is estimated to 8.135×10^{-5} mm barrer^{-1}. According to our results, in order to have a negligible interference of the electrolyte to oxygen transfer compared to the resistance of the sample, the same stirring speed was maintained for further investigations, which is a reasonable assumption since the resistance to oxygen transfer of the polymer samples used in this work was between 0.001 and 0.18 mm bar^{-1}.

$$\left(\frac{t}{Dk}\right)_{eq} = \left(\frac{t}{Dk}\right)_{sample} + \left(\frac{t}{Dk}\right)_{electrolyte} \quad \text{(Eq. 5)}$$

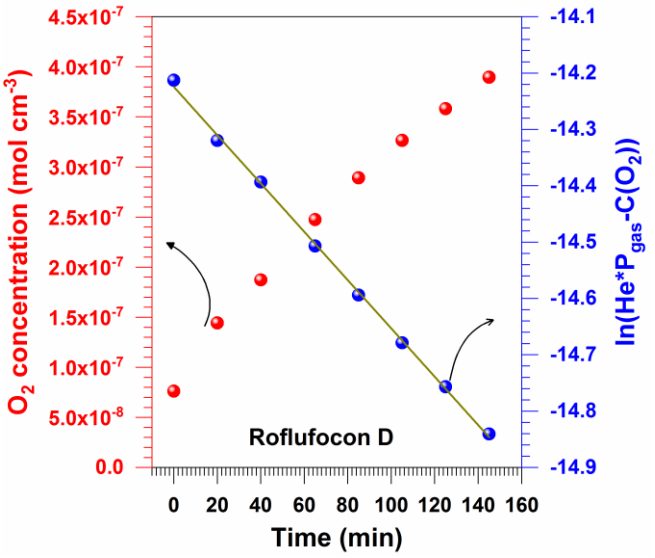

Figure 5. Variation of oxygen concentration and ln(He*Pair-O2(t)) as a function of time for the Roflufocon D at $P(O_2)$ = 1.5 bar in the gas compartment at 35 °C.

We next performed the permeability measurements at 1.5 bar with the previously determined stirring speed. Based the results presented in Figure 5, the oxygen permeability of the investigated material Roflufocon D was evaluated to be 86 barrer and a relative standard deviation (*RSD*) was estimated to be 6%.

Influence of the nature of the polymer material on permeability measurement

Having optimized the experimental conditions for the determination of the oxygen permeability by the designed 3D-printed cell, we sought to study more carefully the impact of the physical and chemical properties of the polymer material on oxygen permeability. To this end, the oxygen permeability measurement was studied for the standard PMMA (methyl polymethacrylate), a soft polymer material herein referred to as MED6010 (see the Experimental Section). The oxygen pressure in the gas compartment was fixed at 1.5 bar for MED6010 and 3 bar for the PMMA in order to have a measurable increase of oxygen concentration in the electrolyte compartment while preventing possible leak. As shown in Figure 6, the increase of oxygen concentration in the electrolyte compartment is faster with MED6010 than with PMMA. The extracted quantitative data are resumed in Table 1. Overall, the oxygen permeability that follows the trend MED6010 > Roflufocon > PMMA is slightly influenced by the value of the oxygen pressure in the gas compartment (1.5 versus 3 bar). It can therefore be briefly summed up that, for low permeability polymer material such as PMMA, a working pressure of 3 bar in the gas compartment is considered optimal to allow a sufficient and measurable flow rate into the liquid chamber. For a polymer material with medium permeability such as Roflufocon D, a high or low pressure (3 and 1.5 bar) can be used provided that the permeability calculation is performed using the data measured in the no-leak region. Finally, for high permeability polymer materials such as MED6010, a low gas pressure of 1-1.5 bar should be used to

avoid a rapid increase in pressure in the electrolyte compartment and prevent possible leaks.

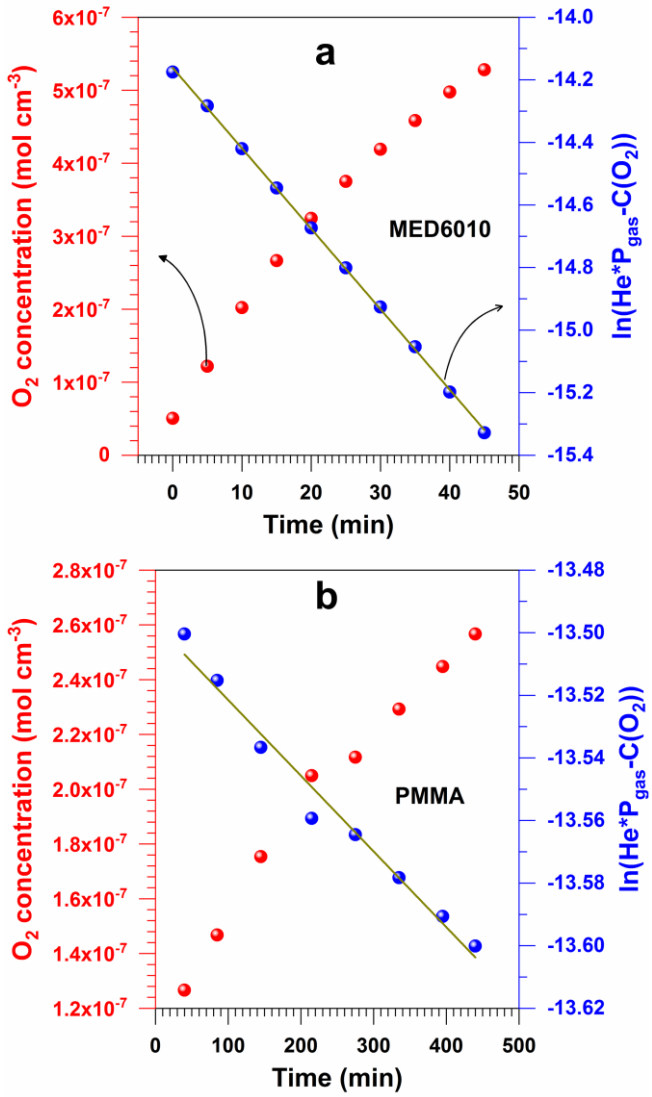

Figure 6. Variation of oxygen concentration and ln(He*Pair-O2(t)) as a function of time for (a) the MED6010 at P_{gas} = 1.5 bar and (b) PMMA at P_{air} = 3 bar and at 35°C.

Table 1. oxygen permeability values measured at different oxygen pressure in the gas compartment for the polymer samples PMMA, Roflufocon D and MED6010. P_{gas} is the oxygen pressure in the gas compartment. Standard deviation is determined from $n \geq 3$.

Materials	Present electrochemical method		Time-lag method
	P_{gas}(bar)	Permeability (barrer)	
Roflufocon D	1.5	89 ± 6	111 ± 25
	3	86 ± 5	
MED6010	1.5	305 ± 17	327 ± 9
	1	294 ± 18	
PMMA	3	4.0 ± 0.2	0.5 ± 0.2

Validation of the developed method: Comparison with Permeability measurements obtained by the time-lag method

The measurement of oxygen permeability by the chronoamperometry method makes it possible to approximate the actual operating conditions of contact lenses where the physiological liquid is in contact with the inner surface while the gaseous oxygen is in contact with the outer surface of the lens. Exposing the sample to liquid on one side and dry gas on the other side leads to a sample that is partially saturated with water that can change its overall permeability. We next aimed to compare, in Figure 7 (and Table 1), the oxygen permeability measured by our developed electrochemical set up to the values obtained by the classic time-lag method fully performed in dry conditions. This enables to validate our developed strategy.

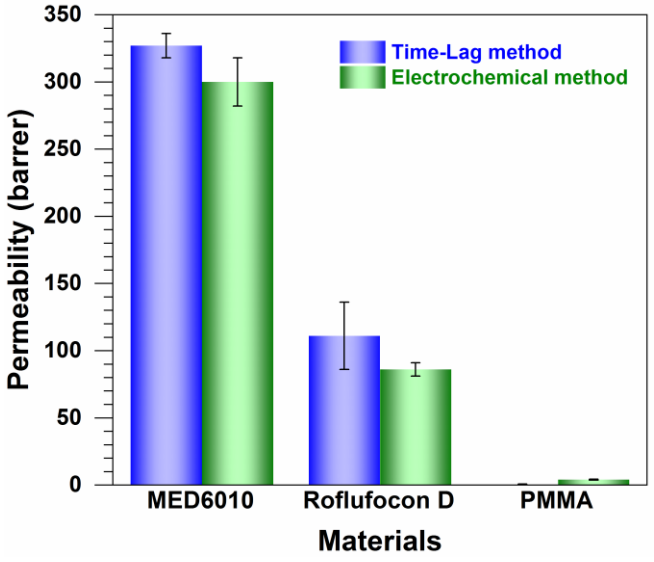

Figure 7. Comparison between the oxygen permeability measured using the developed electrochemical setup and the classic time-lag method. Error bars represent the standard deviation (SD, $n \geq 3$).

The findings indicate that for both MED6010 and Roflufocon D, the measured oxygen permeability is higher for the time lag method (+9 % for the MED6010 and +20 % for the Roflufocon D) whereas it is the contrary for PMMA. It is worth of mentioning that not only the developed method enables achieving valid values for the first two samples in comparison to the gas-gas-method, but also results in a O_2 permeability value in accordance with the value of 100 barrers indicated by the manufacturer Contamac™ for the Roflufocon D. Those outcomes validate the proposed methodology with 3D printing cell. Furthermore, the value evaluated for the PMMA material with the time-lag method is 8 times lower than that determined by the electrochemical method. This observation could be due to the absorption of electrolytes by the sample, which increases or decreases the permeability of the sample when the experiments take place under liquid conditions. Knowing that the permeability of the electrolyte measured by the electrochemical technique is about 40 barrer, if the permeability of the sample to oxygen is higher than that of the oxygen in the interstitial liquid, the

saturated (or partially saturated) sample will have a lower permeability and vice versa. Nevertheless, when the permeability of the sample material is lower than the permeability of oxygen in interstitial liquid, the humidity saturated sample will have a higher permeability than the permeability measured in a dry environment (time-lag method). This is known as oxygen affinity to the aqueous or non-aqueous phase inside the material that is saturated or partially saturated with water.[17] Furthermore, the enhanced permeability of PMMA that is partially saturated with water was related to the higher permeability of oxygen in interstitial liquid compared to that in PMMA. The same effect was reported for hydrogel based materials[17] at low saturation ratio. For the conventional hydrogel, the oxygen is transported through the aqueous phase because it has lower affinity to the polymer matrix. For silicone-based hydrogel, oxygen transport through the aqueous phase is not affected while the increased oxygen permeability of the polymer matrix increases the overall permeability.

The permeability measurement using the time-lag method requires a vacuum step for sample degassing which was not possible to perform on the gel-like samples. Therefore, the present electrochemical method represents an advantage for the measurements on the gel samples since the degassing is rather performed using nitrogen bubbling into the electrolyte solution so no vacuum degassing step required.

For the time-lag method, the O_2 concentration is measured automatically and continuously by a pressure transmitter, while the electroanalytical measurement requires an additional manual electrochemical measurement. However, the electroanalytical method is a "cost-effective" alternative to the gas-to-gas method because the diffusion cell is manufactured by a 3D printing process from an inexpensive polymer, and lower O2 pressure can be used. The electroanalytical method is more sensitive and allows to measure permeability from 10 to 100 times lower. A further advantage of the diffusion cell is the permeability measurements under conditions close to lens wear with the possibility of testing curved materials, whereas time-lag measurements are only performed on flat materials.

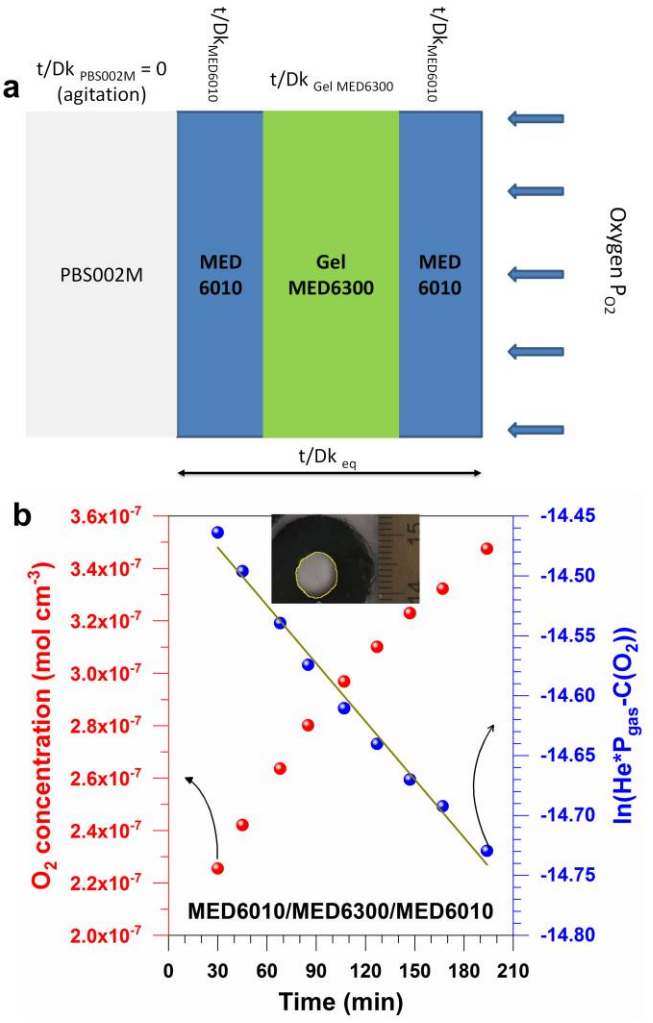

Figure 8. (a) Schematic representation of the MED6010/GelMED6300/MED6010 stack to determine the oxygen permeability of the GelMED6300 and (b) Variation of oxygen concentration and ln(He*P_{gas} – C(O2)) as a function of time for the MED6010/GelMED6300/MED6010 stack at P_{gas} = 1.5 bar and 35°C.

Application of the developed strategy to gel samples

After demonstrating the ability to use electrochemical method with the 3D-printed cell developed to measure the oxygen permeability on polymer materials, we next applied it to gel samples. Indeed, the previous results clearly pointed out the limitation of the time-lag method. Herein, the studied gel MED6300 was encapsulated between two MED6010 materials (with known thickness and permeability). The equivalent oxygen diffusion resistance of the three layers can be calculated considering resistances in series as shown in Figure 8a. The electrolyte oxygen transfer resistance is negligible by means of magnetic stirring so that the measured permeability is only related to the oxygen diffusion through the system of device MED6010/GelMED6300/MED6010 as expressed in Eq. 6. It should be mentioned that only the electrochemical method allowed the permeability measurement of those gel samples, which was not possible using other methods such as the-gas-to gas method. After preliminary trials with different pressures, we come up with the choice of an oxygen pressure at 1 and 1.5 bar

in the gas chamber, which allows preventing fast pressure increase in the gas compartment. The oxygen permeability of the gel material was evaluated to be 211 and 204 barrer at 1 and 1.5 bar, respectively (Table 2).

$$\left(\frac{t}{Dk}\right)_{measured} = \left(\frac{t}{Dk}\right)_{MED6010} + \left(\frac{t}{Dk}\right)_{GelMED6300} \quad \text{(Eq. 6)}$$

Table 2. Oxygen permeability measurements on the MED6010/GelMED6300/MED6010 multilayer and calculated oxygen permeability for the GelMED6300. Standard deviation is determined from $n \geq 3$.

Materials	P_{gas}(bar)	Permeability (barrer)
MED6010/GelMED6300/MED6010	1	159 ± 10
	1.5	156 ± 9
GelMED6300	1	211 ± 12
	1.5	204 ± 12

Conclusion

In this work, a 3D-printed electrochemical cell was fabricated in order to implement an electroanalytical method for the determination of the oxygen permeability in lens-based polymer materials. The optimized conditions utilize the simple Cottrell equation to quantify the dissolved oxygen concentration in the interstitial liquid region, thus accessing the oxygen permeability of different flexible and rigid polymer-based materials (Roflufocon D, MED6010 and PMMA) as well as the gel-type materials (MED6300) which was not possible using the time-lag method due to the required vacuum degassing step in dry condition. Compared to the time-lag method, the developed methodology has the advantage of measuring the oxygen permeability under conditions similar to those of scleral and contact lens (samples saturated or partially saturated with humidity). The second merit is also the elimination of the edge effect that is generally noticed in the case of the classic Fatt polarography method. Our findings revealed that, to be effective, it is necessary to ensure sufficient homogenization of the electrolyte in order to eliminate or minimize the resistance to oxygen diffusion and solubility. In addition, the oxygen pressure in the electrolyte chamber must be low enough to prevent a rapid increase of the pressure in the electrolyte compartment. For the samples studied herein, an oxygen pressure in the gas compartment of 1.5 bar would be recommended and can be used as reference value for measuring other samples with different permeability values. Compared to the automated time-lag method, the present electrochemical approach requires manual measurements at each defined time step, but it is however more adequate to measure oxygen permeability under real lens wearing conditions than the standard polarography method that utilized the toxic mercurous. Also, oxygen gas is in contact with the external side of the material while the electrolyte (similar to tears in the case of scleral and contact lens wear) is in contact with the internal side. In addition, since the electrodes are not in a close contact with the sample to be characterized, edge effects can be overcome.

Experimental Section

Preparation of the polymer materials

Different types of polymer materials were studied in this work. The rigid polymer material Roflufocon D of CONTAMAC in its Optimum Extra version, and PMMA (methyl polymethacrylate) obtained from VISTA-OPTICS both used as received. A soft polymer material called MED6010 and a gel-like material called MED6300 purchased from NUSIL in the form of elastomer kit and procedure of fabrication. The typical procedure from the elastomer kit consisting in mixing the elastomer base (vinyl-terminated polydimethylsiloxane (PDMS, linear chains, Part A) with the curing reagent (short chains presenting SiH functions, Part B) to react with the vinyl groups in presence of platinum catalyst at the speed of 500 rpm for 1 h at room temperature. To make the material MED6010, parts A and B were mixed in 1:1 ratio. The mixture was then poured into a Petri dish and cured at 150 °C for 30 min in a convection oven. The resulting film, about 0.5 mm thick, was cut into disc with a diameter of 2 cm. In the case of the MED6300 gel, parts A and B were mixed in 3:1 ratio. Then the mixture was poured between two homemade MED6010 polymer layers, and polymerized for 5 h at 140 °C in a convection oven as recommended by the supplier to form completed reaction in the final gel.

Electrochemical measurements

The permeability experiments by electrochemical method were carried out in phosphate buffer saline solution from Sigma-Aldrich (PBS, 0.02 M, pH = 7.3). The current magnitude in this study is in micro-scale (Figure 9a), and the uncompensated “solution resistance” determined by the method of the electrochemical impedance spectroscopy was 101 Ω. So, the expected iR-drop is 101*1 = 101 µV = 0.1 mV, which is negligible compared to the applied value of hundreds of mV. Before measurements, the polymer material was immersed in PBS for at least 12 h and then fixed in the diffusion cell. The liquid chamber was then completely filled with PBS (9 ± 0.3 mL) and outgassed by N_2. The electrolyte chamber was then isolated from the ambient air using two closing valves to prevent oxygen leak (see Figure 1). Oxygen flux (with purity ≥99.5%) was sent through the inlet of the gas chamber and the pressure was adjusted by means of a pressure regulation valve at the gas outlet of the gas chamber. In this work, after preliminary tests, pressures of 1, 1.5, and 3 bar (± 0.02 bar) were considered depending on the measured permeability value. The entire electrochemical measurements were performed in a temperature-controlled chamber at 35 ± 1 °C to mimic the eye surface temperature.

LSV measurement

The electrochemical characterization of oxygen reduction at the Pt electrode was first evaluated by linear sweep voltammetry (LSV) in the electrolyte compartment with the three-electrode cell using an OrigaStat OGS100 potentiostat (Origalys). The cell was situated in a Faraday cage. LSV was conducted from the open circuit potential (OCP) to -0.9 V vs Ag/AgCl at a scan rate of 10 mV s^{-1} (Figure 9a). Dissolved oxygen is reduced at the Pt cathode surface according to the reaction: $O_{2(dis)} + 4H^+_{(aq)} + 4e^- \rightarrow 2H_2O_{(l)}$.

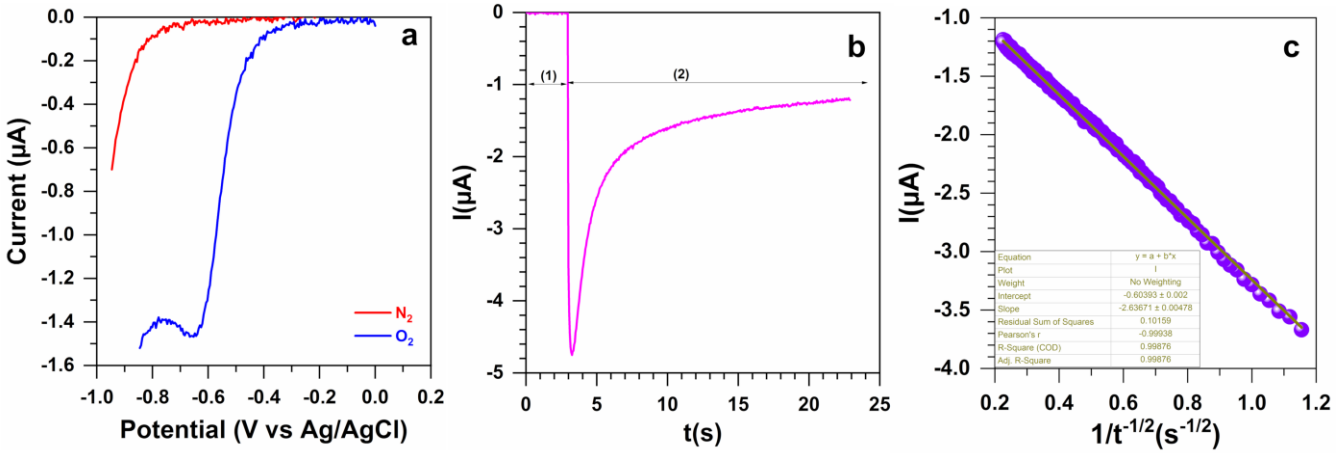

Figure 9. (a) LSV recorded at 10 mV s^{-1} in the electrochemical cell at Pt electrode (1.6 mm diameter) in a closed biological electrolyte (PBS, 0.02 M, pH7.3, 35 °C): in the absence (red curve) and presence of oxygen (blue curve). (b) Two steps CA experiments: (1) OCP stabilization and (2) CA at -0.75 V vs Ag/AgCl. (c) Cottrell plot.

Permeability measurements from electroanalytic technique

The chronoamperometry technique consists of applying voltage steps at the Pt electrode and recording the transient current response of dissolved oxygen in the liquid chamber as a function of time (Figure 9b). Before experiment, the three-electrode cell was stabilized for 3 s at the OCP and then, a potential of -0.75 V vs Ag/AgCl was applied to the Pt electrode for 20 s to measure the reduction current of dissolved oxygen. On the basis on the profile of the LSV in the absence and presence of oxygen, different electrode potentials were probed but the above value of -0.75 V vs Ag/AgCl was the best compromise. Similar value was previously used.[6f,6g,18] The measurements were performed at interval times to monitor the oxygen concentration as a function of time. During the reduction of the oxygen in the close vicinity of the electrode surface, a concentration gradient is created across the electrolyte between the bulk of the solution and the electrode surface, and the measured transient oxygen reduction current becomes diffusion limited. Therefore, faradaic current near the electrode surface decays over time as the mass transport limit is reached. These currents provide a typical exponential decay curve, which is described by the Cottrell equation (Eq. 7).[19] The slope of the Cottrell plot (Figure 9c) is determined from the linear variation of the absolute value of the measured current versus the inverse square root of time ($1/t^{1/2}$) and allows determining the oxygen concentration in the bulk electrolyte C(mol cm^{-3}). The oxygen concentration variation as a function of time in the electrolyte chamber described by Eq. 8 allows establishing the relationship between O_2 permeability (Perm) and the pressure of the gas (P_{gas}), Eq. 9. The plot of $\ln(He \times P_{gas} - C)$ *vs* t leads to the determination of Perm for a given sample transfer surface (S) and the electrolyte volume in the liquid chamber (Eq. 10). Then, the permeability can be expressed in barrer according to Eq. 11.

$$I = nACF\sqrt{\frac{D}{\pi t}} = \left(nACFD^{1/2}\pi^{-1/2}\right)\frac{1}{\sqrt{t}} \qquad \text{(Eq. 7)}$$

$$\frac{dC}{dt} = Perm\left(P_{gas} - \frac{C}{He}\right)\frac{S}{V} \qquad \text{(Eq. 8)}$$

$$\ln\left(He \times P_{gas} - C\right) = -\left(Perm\frac{S}{He \times V}\right)t + \ln\left(He \times P_{gas} - C_0\right) \qquad \text{(Eq. 9)}$$

$$Perm = \frac{slope \times He \times V}{S} \qquad \text{(Eq. 10)}$$

$$1barrer = 3.35 \times 10^{-16}\frac{mol \times m}{m^2 \times s \times Pa} \qquad \text{(Eq. 11)}$$

Where I(A) is the measured current, n is the overall transferred number of electrons per molecule of O_2 oxygen (n = 4), C(mol cm^{-3}) is the bulk concentration of O_2 in the electrolyte, F(= 96485 C mol^{-1}) is the Faraday constant, D(= 2.7×10^{-5} cm^2 s^{-1}) is the diffusion coefficient of O_2 in water at 35 °C, A(cm^2) is the area of the electrode, t(s) is the time, V(cm^3) is the electrolyte volume, He(mol cm^{-3} bar^{-1}) is the Henry constant, S(cm^2) is the sample surface exposed to O_2, and the "slope(s^{-1})" is the slope of the variation of $\ln(He\times P_{gas} - C)$ as a function of time.

Permeability measurements using gas-to-gas (time-lag) method

Permeability measurements by the time-lag method were carried out using a dual-chamber apparatus placed in a temperature controlled chamber at 35 °C as shown in Figure 10. The sample is mounted between two chambers: the inlet and the outlet chamber. The device was initially degassed under vacuum overnight, and the inlet chamber was filled with oxygen at 3 bar (maintained constant during the measurement, P_{inlet}) to measure the oxygen permeability. The passage of oxygen through the polymer material increases the pressure in the outlet chamber. The pressure P_{outlet} is measured as a function of time. The slope of the variation of P_{outlet} in pseudo-stationary regime allows the oxygen permeability to be calculated using the Eq. 12. All the experimental measurements were performed at least three times, and the results were reproducible.

$$Perm\left[mol_{STP} \times m^{-1} \times s^{-1} \times Pa^{-1}\right] = \frac{V \times e}{A \times R \times T \times P_{inlet}}\frac{dP_{outlet}}{dt} \qquad \text{(Eq. 12)}$$

Where Perm is the permeability (barrer), V(m^3) is the volume of the outlet chamber, e(m) is the sample thickness, S(m^2) is the area of the sample surface exposed to oxygen, R(= 8.314 J K^{-1} mol^{-1}) is the gas constant, T(= 273.15 + θ, where θ is the temperature in °C) represents the temperature in Kelvin, and P_{inlet}(= 3 bar) is the oxygen pressure in the inlet chamber.

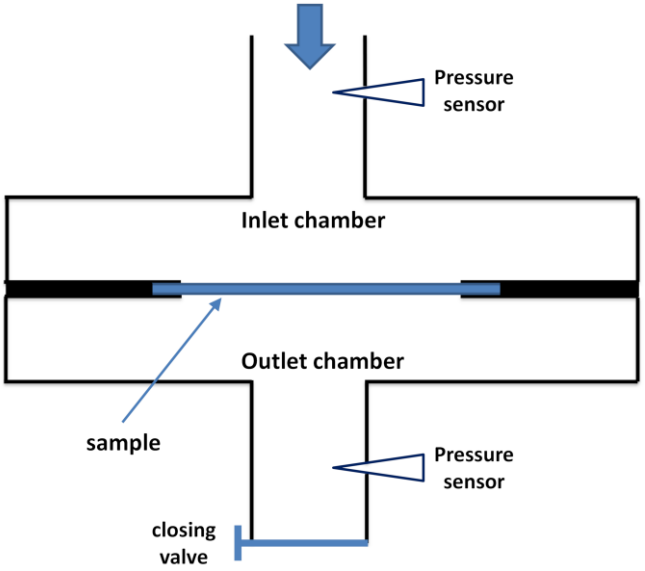

Figure 10. Simplified schematic representation of the time-lag measurement method (in a temperature-controlled chamber at 35 ± 1 °C).

Acknowledgements

This work has been Co-funded by ANRT (French National Association for Research and Technology) under the grant number CIFRE N° 2017/0028 and Ophtimalia SAS, 5 esplanade Anton Philips Campus EffiScience, 14460 Colombelles, France.

Conflict of Interest

The authors declare no conflict of interest.

Keywords: lens material • electroanalysis • oxygen permeability • oxygen reduction reaction • polymer membrane

References

[1] a) B. Tan, V. Tse, Y. H. Kim, K. Lin, Y. Zhou, M. C. Lin, *Cont. Lens Anterior Eye* **2019**, *42*, 366-372; b) R. B. Mandell, K. A. Polse, I. Fatt, *Arch. Ophthalmol.* **1970**, *83*, 3-9; c) K. W. Pullum, F. J. Stapleton, *CLAO J.* **1997**, *23*, 259-263; d) B. A. Holden, D. F. Sweeney, A. Vannas, K. T. Nilsson, N. Efron, *Invest. Ophthalmol. Vis. Sci.* **1985**, *26*, 1489-1501; e) B. A. Holden, G. W. Mertz, *Invest. Ophthalmol. Vis. Sci.* **1984**, *25*, 1161-1167; f) V. Compañ, C. Oliveira, M. Aguilella-Arzo, S. Mollá, S. C. Peixoto-de-Matos, J. M. González-Méijome, *Invest. Ophthalmol. Vis. Sci.* **2014**, *55*, 6421-6429; g) V. Compañ, M. Aguilella-Arzo, T. B. Edrington, B. A. Weissman, *Optom. Vis. Sci.* **2016**, *93*, 1339-1348; h) M. K. Walker, J. P. Bergmanson, W. L. Miller, J. D. Marsack, L. A. Johnson, *Cont. Lens Anterior Eye* **2016**, *39*, 88-96.

[2] E. S. Bennett, B. A. Weissman, *Clinical Contact Lens Practice*, Lippincott Williams and Wilkins, Philadelphia, USA, **2004**.

[3] M. D. SARVER, D. A. BAGGETT, M. G. HARRIS, K. LOUIE, *Optom. Vis. Sci.* **1981**, *58*, 386-392.

[4] M. C. Madigan, P. L. Penfold, B. A. Holden, F. A. Billson, *Cornea* **1990**, *9*, 144-151.

[5] a) R. C. Reid, S. D. Minteer, B. K. Gale, *Biosens. Bioelectron.* **2015**, *68*, 142-148; b) G.-Z. Chen, I.-S. Chan, L. K. K. Leung, D. C. C. Lam, *Med. Eng. Phys.* **2014**, *36*, 1134-1139; c) H. E. Milton, P. B. Morgan, J. H. Clamp, H. F. Gleeson, *Opt. Express* **2014**, *22*, 8035-8040; d) K. Mitsubayashi, T. Arakawa, *Electroanalysis* **2016**, *28*, 1170-1187; e) X. Xiao, T. Siepenkoetter, P. Ó. Conghaile, D. Leech, E. Magner, *ACS Appl. Mater. Interfaces.* **2018**, *10*, 7107-7116.

[6] a) S.-T. Hwang, T. E. S. Tang, K. Kammermeyer, *J. Macromol. Sci., Part B: Phys.* **1971**, *5*, 1-10; b) S. Aiba, M. Ohashi, S. Y. Huang, *Ind. Eng. Chem. Fundamen.* **1968**, *7*, 497-502; c) M. S. Goldenberg, E. Rennwantz, A. Beekman, *International Contact Lens Clinic* **1991**, *18*, 154-162; d) V. Compañ, J. S. Román, E. Riande, T. S. Sørensen, B. Levenfeld, A. Andrio, *Biomater.* **1996**, *17*, 1243-1249; e) V. Compan, J. Garrido, J. A. Manzanares, J. Andres, J. S. Esteve, M. L. Lopez, *Optom. Vis. Sci.* **1992**, *69*, 685-690; f) V. Compañ, E. Riande, J. S. Román, R. Díaz-Calleja, *Polymer* **1993**, *34*, 3843-3847; g V. Compañ, M. L. Lopez, L. Monferrer, J. Garrido, E. Riande, J. San Roman, *Polymer* **1993**, *34*, 2971-2974.

[7] I. Fatt, *Int. Contact Lens. Clin.* **1991**, *18*, 192-199.

[8] G. B. Y. Christie, J. I. Macdiarmid, K. Schliephake, R. B. Tomkins, *Postharvest Biol. Technol.* **1995**, *6*, 41-54.

[9] a L. C. Clark, R. Wolf, D. Granger, Z. Taylor, *J. Appl. Physiol.* **1953**, *6*, 189-193; b L. C. Clark, C. Lyons, *Ann. N.Y. Acad. Sci.* **1962**, *102*, 29-45.

[10] I. Katsounaros, S. Cherevko, A. R. Zeradjanin, K. J. J. Mayrhofer, *Angew. Chem. Int. Ed.* **2014**, *53*, 102-121.

[11] L. W. McKeen, in *Permeability Properties of Plastics and Elastomers (Fourth Edition)* (Ed.: L. W. McKeen), William Andrew Publishing, **2017**, pp. 1-19.

[12] V. Compañ, J. Guzmán, E. Riande, *Biomaterials* **1998**, *19*, 2139-2145.

[13] J. Wichterlová, K. Wichterle, J. Michálek, *Polymer* **2005**, *46*, 9974-9986.

[14] a) E. Katz, *Implantable Bioelectronics*, Wiley-VCH Verlag GmbH & Co. KGaA, Weinheim, Germany, **2014**; b) G. A. Truesdale, A. L. Downing, *Nature* **1954**, *173*, 1236-1236.

[15] a) K. E. Gubbins, R. D. Walker, *J. Electrochem. Soc.* **1965**, *112*, 469-471; b) W. Xing, G. Yin, J. Zhang, *Rotating Electrode Methods and Oxygen Reduction Electrocatalysts*, 1 ed., Elsevier Science and Technology, Poland, **2014**.

[16] B. Debelius, A. Gómez-Parra, J. M. Forja, *Hydrobiologia* **2009**, *632*, 157-165.

[17] A. Ledwith, in *Encyclopedia of Materials: Science and Technology* (Eds.: K. H. J. Buschow, R. W. Cahn, M. C. Flemings, B. Ilschner, E. J. Kramer, S. Mahajan, P. Veyssière), Elsevier, Oxford, **2001**, pp. 7341-7351.

[18] D. Obendorf, M. Wilhelm, *Anal. Chem.* **2003**, *75*, 1374-1381.

[19] a) A. J. Bard, L. R. Faulkner, *Electrochemical Methods: Fundamentals and Applications*, 2nd ed., John Wiley & Sons, Inc., USA, **2001**; b) E. Gileadi, *Electrods Kinetics for Chemists, Chemical Engineers, and Materials Scientists*, Wiley-VCH, New York, N Y, USA, **1993**.

Entry for the Table of Contents

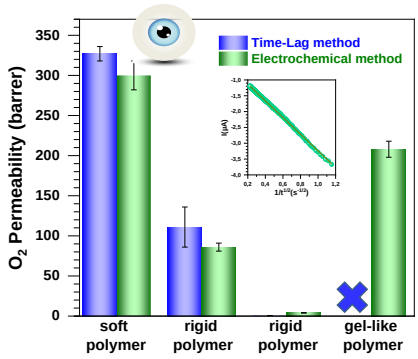

Dry lens or wet lens? : O_2 permeability of a lens material is different when measuring in dry or in wet conditions. The electrochemical method allows accurate measurements of O_2 reduction under similar real lens wear conditions and offers a viable alternative to the classic Time-Lag method operating in dry environment. Permeability depends on O_2 affinity to the aqueous or non-aqueous phase inside different type of polymer materials.